Parametric Amplification and Wavelength Conversion in Dual-Core Highly Nonlinear Fibers

Vitor Ribeiro, *Senior Member, OSA,* Áron D. Szabó, Ana M. Rocha, Chandra B. Gaur, Abdallah A. I. Ali, Yves Quiquempois, Arnaud Mussot, Géraud Bouwmans and Nick Doran

***Abstract*—In this paper we experimentally show parametric amplification and wavelength conversion in a custom manufactured dual-core highly nonlinear fiber. On-off gain > 10 dB and conversion efficiencies between -1 and -8.5 dB were measured for both cores. The estimated effective nonlinear parameter for the cores of the fiber are $6.6\ \mathrm{W^{-1}\,km^{-1}}$ and $6.3\ \mathrm{W^{-1}\,km^{-1}}$, while the zero-dispersion wavelength for the individual cores is shown to be relatively close from each other. Furthermore, complementary analytical and numerical results show that coupled cores fiber optical parametric amplifier offer the potential of wide-band gain even when they have significantly distinct zero-dispersion wavelengths.**

***Index Terms*—Parametric amplifiers, spatial division multiplexing.**

I. Introduction

ALL-optical signal processing in dual-waveguide structures has since long back attracted great attention. It was already in the early 1980s with the introduction of the theory for nonlinear directional coupler [1], [2], that dual-coupled waveguide devices started to pave their way as a useful way for possible applications in the field of all-optical signal processing. The relative fast response of the third order susceptibility χ^3 allows to create a fast phase-matching imbalance between waveguides allowing applications, such as fast femtosecond soliton switching [3]–[6] and parametric amplification/squeezed light generation [7]. Nevertheless the promising application of dual-waveguide devices for all-optical signal processing applications took long to take off. The first known reported experimental demonstration of a dual-core fiber was in the mid 1980s [8], where demonstration of stimulated four-wave mixing (FWM) and Raman scattering was performed. Nevertheless further experimental studies are scarce and it was just more recently, that more experiments on dual core fibers were performed [9]–[13]. Moreover the current development of photonic integrated circuits (PICs) based in SI_3N_4 [14] and multicore fibers creates the perfect opportunity to build devices based in this structures.

There has been an increased interest on doing all-optical signal processing applications in dual-core highly nonlinear fibers (DC-HNLFs) and theoretical findings [15]–[20], suggest that using the inherited phase-mismatch, between the two supermodes (odd and even) of a dual-core fiber given by 2 times the coupling parameter C of the fiber [21], it is possible to compensate the induced phase-mismatch of the pump on the signals leading the fiber optical parametric amplifier (FOPA) to create a flat gain spectrum over a wide bandwidth and with exponential gain increase over the length of the fiber [15]. This theory is in agreement with previous published work on modulation instabilities in DC-HNLFs [22], however [15], [16] intended to provide the analytical tools for a more convenient study of this schemes and for a rapid deployment of this devices. Interesting competing schemes such as the dual-pump FOPA [23], [24], also provides gain spectral flatness, however the wavelength difference between pump wavelengths, often falls within the bandwidth of the Raman-gain spectrum. Therefore if the two pumps cannot maintain equal power levels along the length of the fiber, FWM efficiency is reduced, even though total power remains constant [25]. This does not occur with the dual-core FOPA (DC-FOPA), since the two pumps propagating in two spatial modes, occupy the same frequency mode.

In this paper we experimentally demonstrate parametric amplification and all-optical wavelength conversion in an weakly-coupled DC-HNLF, extending our recent OFC 2021 paper [26]. We extend the work published in [26] by providing more details about the DC-HNLF, including a figure of its cross-section (Fig. 2), details about the dispersion characteristics of both cores of the DC-HNLF, including 2^{nd}, 3^{rd} and 4^{th} order dispersion wavelength dependent parameters (Fig.4) and results about parametric amplification in a DC-HNLF (Fig. 5). DC-HNLF can work in 2 regimes, coupled and uncoupled. In practical terms the latter regime is weakly coupled since 2 cores, built in the same fiber, will in general have some coupling between them. We prefer throughout the paper to use the term weakly coupled in order to be as rigorous as possible. The experimental results study the case of weakly coupled FOPA and we wanted to analyze numerically using same physical parameters of the fibre, i.e. nonlinear parameter, and experimentally obtained 3^{rd} order dispersion, the impact in performance of having 2 cores with distinct zero-dispersion wavelength (ZDW). Therefore we add a discussion section in Section IV where parametric amplifiers based on DC-HNLF in the coupled [15] regime are numerically assessed. Experimental

Vitor Ribeiro (email:v.ribeiro@aston.ac.uk), Abdallah A. I. Ali and Nick Doran are with Aston Institute of Photonic Technologies, Aston University, Birmingham, UK.

Yves Quiquempois, Arnaud Mussot and Geraud Bouwmans are with Univ. Lille, CNRS, UMR 8523 - PhLAM - Physique des Lasers, Atomes et Molecules, F-59000 Lille, France

Ana M. Rocha is with Instituto de Telecomunicacoes and Universidade de Aveiro, Campus Universitario de Santiago, 3810-193 Aveiro, Portugal

Áron D. Szabó is with Aston Institute of Photonic Technologies, Aston University, Birmingham, UK. Now with Sigma Technology Hungary Ltd., Kozraktar str. 30-32., Budapest H-1093, Hungary

Chandra B. Gaur is with Aston Institute of Photonic Technologies, Aston University, Birmingham, UK. Now with SubCom LLC, 250 Industrial Way W, Eatontown, NJ 07724, USA

Manuscript received April 19, 2005; revised August 26, 2015.

results show that the ZDW of the cores of the DC-HNLF are slightly different and separated by 5 nm. A common concern that can be presented for future designers of parametric amplifiers based on coupled DC-HNLF is that if this difference may compromise the performance and realization in the coupled regime scenario. In order to answer that question in section IV we have used same fibre design parameters, relatively to the ones obtained experimentally in the weakly-coupled core scenario and analyzed the performance of the parametric amplifier, sweeping several design parameters of the DC-HNLF. With this discussion we hope to show the extreme flexibility of this type of amplifiers and motivate experts in the field to pursue the goal to manufacture this outstanding type of amplifiers. This work is already underway in our laboratory with a new sample of a coupled DC-HNLF already manufactured for further experiments. In our experimental results we achieved > 10 dB on-off (O/O) gain for both cores and wavelength conversion efficiencies > -8.5 dB. In this demonstration we used our first sample of a DC-HNLF, where the cores happened to be weakly-coupled . The present sample is suitable for stable polarization diversity schemes and has potential for multicore fiber optical parametric amplification in a spatial division multiplexing (SDM) link. The experimental results of Section III and numerical calculations of section IV were both performed in a a Mach-Zhender (MZ) interferometer arrangement. MZs are known to cause phase drifts and stabilization problems mostly because the cores/waveguides in both arms of the interferometer are relatively far apart from each other, leading a gradient in temperature to cause deterministic and non-deterministic phase differences between cores/waveguides. Having both cores/waveguides separated by a few micrometers, can ease stabilization of MZ interferometer, decreasing skew between cores/waveguides of the weakly coupled DC-HNLF, when compared to two separated fibres as shown in [27]. For FOPAs based on polarization diversity schemes these phase-differences will be dealt by the receiver the same way as a delay caused by polarization mode dispersion (PMD). Moreover the receiver has a limited range of PMD/delay (≤ 50 ps [28]) that can be compensated over several fibre spans. If the FOPAs in the link accumulate delay it will decrease the range of the propagation distance of the polarization diverse multiplexed signal. This has been a concern in some works related with FOPAs where polarization diversity was addressed (see for example [29]). Phase-shifters can compensate this delay, but the range for which it can be compensated is limited in most cases to a few π radians, after which the service must be disrupted and restarted again. While polarization diversity is not the sole objective of this work, but also as a first step in order to tailor dispersion and nonlineartiy for a future coupled-core amplifier [15], [16] , the work in [27] proves the advantages of using it, with that purpose as well, or for a spatial diverse multiplexed link using a spatial diverse FOPA. The cores of this DC-HNLF were built in the same preform, in order to have very similar dispersion/nonlinearity properties. We believe that future samples, with additional improvement in manufacture process, will allow us to fabricate cores with very identical ZDWs and dispersion profile, opening the way for a wide range of applications in nonlinear fibre optics science. Moreover dispersion fluctuations in multicore fibres are inherently not independent , increasing probability to have both cores with similar average ZDW (see for example a related study in [30]). One of the issues of the very elegant polarization diverse design proposed in [29] is that the zeros of dispersion of the X and Y polarization axis of the polarization maintaining HNLF can be separated by $> 10\,\mathrm{nm}$ [31], leading into difficulties in order to match gains for both polarization modes. The solution provided in this paper match the elegance of [29], while offering better prospects of achieving similar dispersion properties and gains for both polarization modes.

This paper is organized as follows. In section II we introduce the experimental setup. In section III we present the characterization of the fiber and the experimental results related with wavelength conversion and parametric amplification in an weakly-coupled DC-HNLF. In section IV we discuss the obtained results and analyze the effect of distinct ZDWs on the gain and bandwidth of a coupled DC-HNLF. In section V we conclude the paper.

II. Experimental setup

Fig. 1 shows the experimental setup. A seed laser named as the signal laser is combined with a pump laser using a 0.2 nm tunable pass-band filter, comprising a fiber Bragg grating and two circulators. The signal is injected through the transmission port and the pump through the reflection port of the fiber Bragg grating, filtering the excess noise of the pump. The pump signal is placed at 1561.5 nm and is phase modulated, in order to broad the spectrum of the pump and therefore mitigate the effect of stimulated Brillouin scattering. To maintain a high nonlinear phase shift, the pump is chopped by an acousto-optic modulator (AOM) with a chopping period of 1 ms and a duty cycle of 8%. Since the coupling into the fiber tip is sensitive to thermo-mechanical instabilities due to heating, the chopping of the pump helped to reduce the average power of the pump and therefore the average power sensitive heating of the fiber tip.

We have used C and L band lasers with below-25 kHz line-width as signal sources. Since the level of signal/pump power at each output of the polarization beam splitter (PBS) is dependent on signal/pump polarization at the input of the PBS we control the polarization of the signal and the pump independently by placing two polarization controllers in the signal and pump paths in order to have identical signal and pump power in both output arms of the PBS. This was monitored by $1\,\%$ tap couplers, conveniently placed after each PBS output. In that case the PBS also ensures co-aligned signal and pump polarization at each output of the PBS and individual polarization controllers (PCs) at each output of the PBS guaranteed optimized alignment with the birefringent axis of each individual DC-HNLF core for maximum FWM conversion efficiency. After propagation through the 300 m DC-HNLF the spectrum and power is monitored individually by an optical spectrum analyzer and $1\,\%$ tap couplers, respectively.

The stack-and-draw technique is used to manufacture the DC-HNLF in this experiment. A preform with germanium doped graded index difference of 30×10^{-3} at maximum, is first

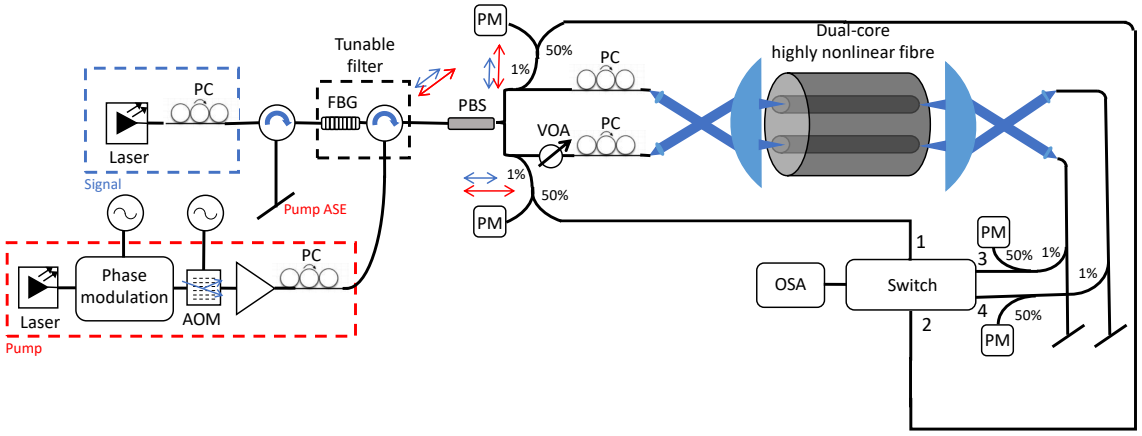

Fig. 1. Setup for parametric amplification and wavelength conversion in a DC-HNLF. Switch ports 1 and 2 monitor input spectrum of core 1 and 2, respectively, and switch ports 3 and 4 monitor the respective output spectrum. PC-polarization controller, OSA-optical spectrum analyzer, PM-power monitor, PBS-polarization beam splitter, FBG-fiber Bragg grating, AOM-acousto-optic modulator and VOA-variable optical attenuator. Similar illustration is provided in [26, Fig. 1] and is replicated here for convenience of the reader.

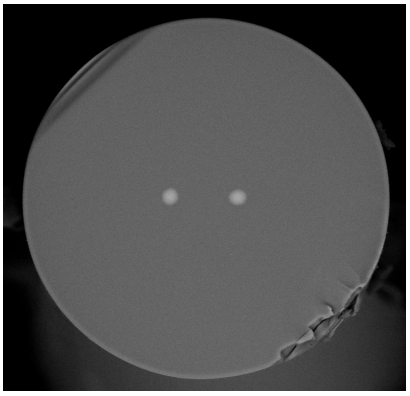

Fig. 2. Cross-section of DC-HNLF. Core to core spacing of 20.4 μm.

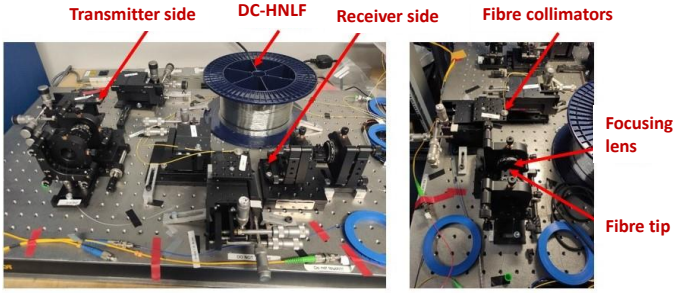

Fig. 3. Laboratory implementation of Fig. 1 related with the coupling mechanism into the DC-HNLF. Identical illustration is provided in [26, Fig.2] and is replicated here for convenience of the reader.

drawn into about two millimeter-thick rods and subsequently assembled in a stack made of pure silica rods and then drawn into a fiber yielding in a DC-HNLF with core radius of ≈ 2.6 μm and 20.4 μm core separation. Fig. 2 shows the cross-section of the fiber. The core radius was chosen in order to have a ZDW somewhere in the C-band, in order to be in accordance with the equipment (lasers and amplifiers) operational bandwidth of our laboratory.

The optical system for coupling-in and coupling-out of the DC-HNLF is custom designed with Zemax software and the overall loss of the coupling system is 3.5 dB, from input to output. The two Gaussian profile fundamental modes of the two single mode fibers at the input of the DC-HNLF are collimated by 1.6 mm diameter coated lenses with 1.81 mm focal length and maximum power tolerance of 3 W. The collimated beams are focused into the cores of the DC-HNLF using a 2.6 mm diameter coated aspherical lens with 2 mm focal length and are hold on a lens holder just before the fiber tip. Each fiber collimator is fixed in 3 degrees of freedom nano-positioning stages, i.e. 2 translation and 1 rotation stages, while the fiber tips of the DC-HNLF and the focusing lenses are fixed on 2-axis translation and tilting holders with axial rotatability, shown in Fig. 3 .

III. Experimental Results

A. Fiber dispersion, nonlinearity characterization and parametric amplification

The dispersion of cores 1 and 2 of the DC-HNLF is shown in Fig. 4. The fiber dispersion of cores 1 and 2 was characterized by an Agilent 86038B photonic dispersion and loss analyzer and by fusion splicing very short and nearly dispersion-less bridge fibres with connectors to the DC-HNLF cores, one at the time. Fig. 4 a) shows the group delay experimental measurements and respective 2^{nd} order polinomial fit. Fig. 4 b) shows the 2^{nd} order dispersion coefficient of the fiber. The difference between the ZDWs of cores 1 and 2 is approximately 5 nm. The 3^{rd} to 4^{th} order dispersion coefficient at the frequency of the pump are shown in Fig. 4 c) to d), using a 2^{nd} order polynomial fit. In our experiment the pump wavelength was 1561.5 nm and accordingly to Fig. 4 b) the ZDW for core 1 is ≈ 1568 nm and for core 2 is ≈ 1563 nm. In that case this would mean the pump would operate in the normal dispersion regime. However this is elusive, since in our experiment we used several meters of single mode fiber (SMF) before coupling the pump wave

into the DC-HNLF. This will lead the average ZDWs for the signal paths of core 1 and core 2 to move towards the shorter wavelengths. However we did not record the accurate number of SMF meters used (> 3 m), so we avoid speculation.

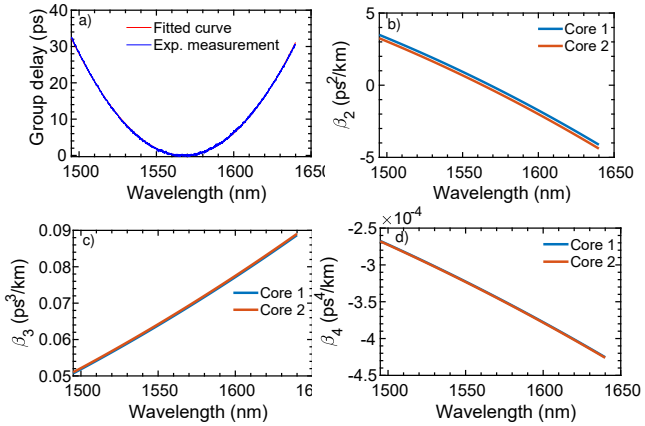

Fig. 4. Measured wavelength dependent dispersion parameters of the DC-HNLF for cores 1 and 2. Fitted curves obtained with a 2^{nd} order polynomial. a) group-delay experimental measurements and fitted curve, b) 2^{nd} order dispersion parameter fit, c)3^{th} order dispersion parameter fit d) 4^{th} order dispersion parameter fit

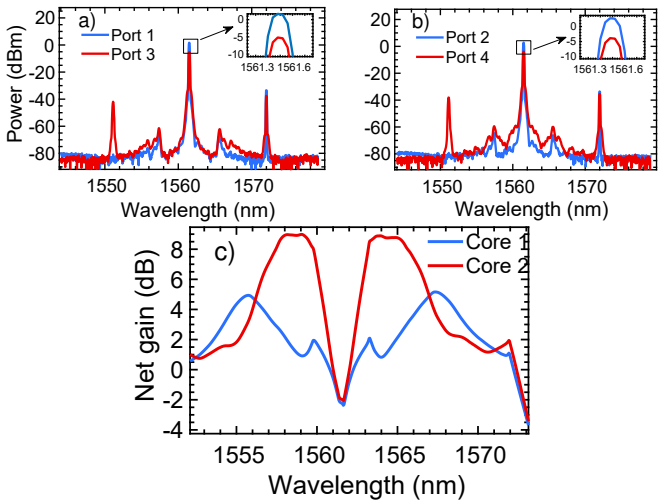

Fig. 5. Power and gain spectrum of core 1 and 2. Input (blue) and output (red) power spectrum of a) core 1 and b) core 2. Gain spectrum of both cores in c). Insets in a) and b) details input and output power losses. In a) and b) signal wave is placed at 1572 nm.

We estimated the nonlinear parameter of the fiber by measuring the O/O gain of both cores and by using a pulsed light source as the pump signal in order to trigger the 3^{rd} order susceptibility (χ^3) of the fiber cores. We set the Yokogawa AQ6370D optical spectrum analyzer (OSA) in time averaging mode and with normal sensitivity setting. However since the repetition rate of the pulsed pump is in the MHz scale, the response time of the detection circuit in the OSA is slow enough that the pulsed pump could be treated as a continuous wave (CW) signal [32]. Since power meters just give access to average power, we estimated the peak pump powers going into the cores by integrating the input power spectrum of the pump fields for cores 1 and 2, over a bandwidth that comprise all the spectrum of the pump. To note that the spectrum shown in Fig. 5 a) and b) is attenuated 23 dB by 1 % plus 50 % tap couplers. Based on this we estimate the peak powers to be $P_{peak_1} = 1.05$ W and $P_{peak_2} = 1.34$ W, for core 1 and 2, respectively. To note that just a small difference in average power of 20 mW will result in peak power difference of more than 200 mW due to a duty cycle of just 8 %, which is easily neglected when measuring with average power monitors. The total losses, i.e. the losses induced by coupling light in to the DC-HNLF (> 3.5 dB) and other components in the path of the signal from input to output of each individual circuit of core 1 and core 2, can be assessed by inspecting the power of the pump at input and output using the OSA. This is shown in Fig. 5 a) and b), in insets, where core 1 presents a total loss of $\alpha_1 = 6.9$ dB and core 2 presents a total loss of $\alpha_2 = 6.7$ dB. Inspecting Fig. 5, c), obtained by comparing the input and output spectrum [33], it can be seen that the maximum net gain of core 1 is $G_{net_1} = 4.9$ dB and the maximum net gain of core 2 is $G_{net_2} = 8.9$ dB. The difference in net gain is the result of difference in peak power between core 1 and 2, previously mentioned. To assess the O/O gain, i.e. the difference in terms of power between the signals, when the pump is off and on, we have to add the losses of each core to its respective net gain [34]. Therefore $G_{O/O_1} = G_{net_1} + \alpha_1 = 11.8$ dB and $G_{O/O_2} = G_{net_2} + \alpha_2 = 15.6$ dB. To estimate the nonlinear parameters of each individual core we recall a fundamental equation of parametric amplifiers [35], $G_{linear} = \cosh(\gamma P_p L)^2$ or in dB $G_{dB} \approx 8.6\gamma P_p L - 6$ [36], giving the maximum gain of the FOPA, over its whole spectrum, where γ is the nonlinear parameter, P_p is the power of the pump and L is the length of the fiber. Substituting G_{dB} by the on-off gain of core 1 and 2, and their respective parameters, we get

$$\gamma_{1,2_{eff}} = \frac{G_{O/O_{1,2}} + 6}{8.6 P_{peak_{1,2}} L}, \tag{1}$$

this leads to $\gamma_{1_{eff}} = 6.6$ W^{-1} km^{-1}, $\gamma_{2_{eff}} = 6.3$ W^{-1} km^{-1}. Fiber was designed to have a $\gamma_{1,2} = 7.4$ W^{-1} km^{-1}, however since fiber has random birefringence, effective nonlinearity per core is decreased by a factor of $8/9$ [37]. Therefore $\gamma_{1,2} = \frac{9}{8}\gamma_{1,2_{eff}}$, leading to $\gamma_1 = 7.4$ W^{-1} km^{-1}, $\gamma_2 = 7.1$ W^{-1} km^{-1},, which yields in values close to the designed ones.

B. Wavelength conversion

In order to measure wavelength conversion efficiency obtained from the DC-HNLF, we have used continuous wave signals in the C+L-band to demonstrate stable simultaneous nonlinear operation of both cores. Fig. 6, shows the measured power spectrum for different signal wavelengths between 1564 to 1573.6 nm, spaced 1.6 nm, in core 1 and 2. It can be noticed that beyond the pump, signals and the generated idlers, 2 sidelobes due to chopping of the pump appear as first crosstalk components.

The wavelength conversion efficiencies were measured as the difference between the signal and idler power levels in dB. One can see from Fig. 7 that it could be measured conversion efficiencies for both cores, between -1 and -8.5 dB and for

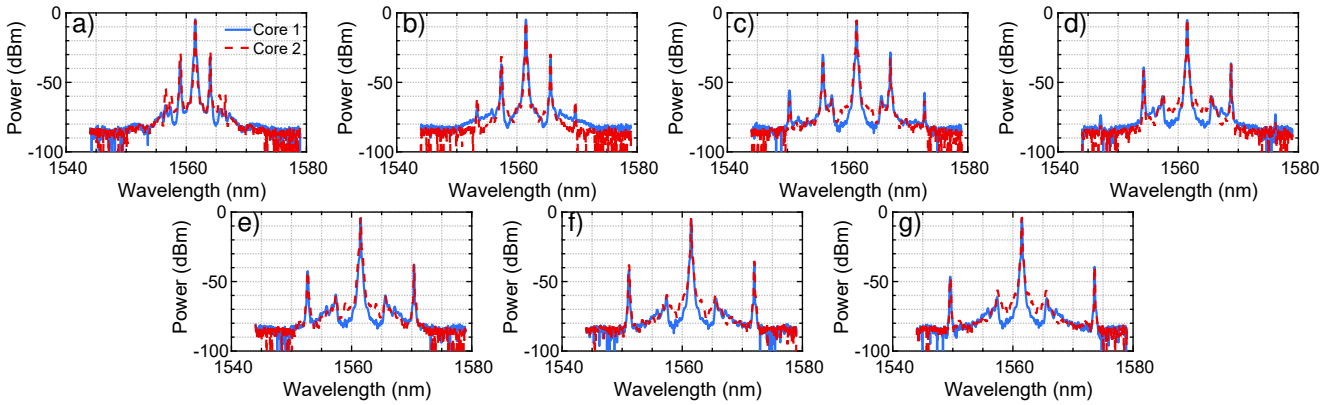

Fig. 6. Subplots a) to g) show output spectrum of cores 1 and 2, obtained by switching ports 3 and 4, respectively, in Fig. 1, for different signal wavelengths. Signal wavelengths are a) 1564 nm, b) 1565.6 nm, c) 1567.2 nm, d) 1668.8 nm, e) 1570.4 nm, f) 1572 nm, g) 1573.6 nm. Similar illustration is provided in [26, Fig.3] and is replicated here for convenience of the reader.

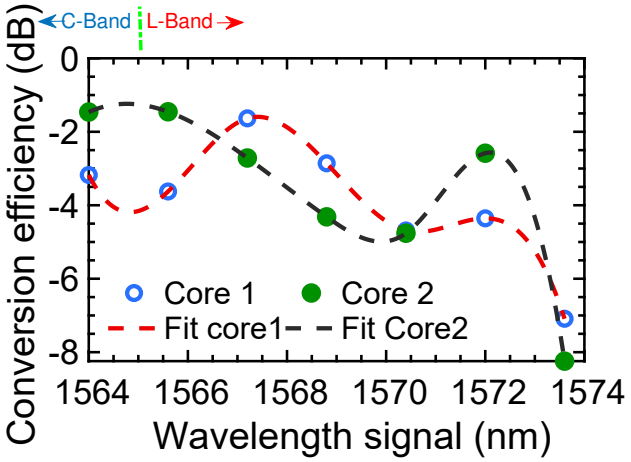

Fig. 7. Summary of the results of Fig. 6. Wavelength conversion efficiency for cores 1 and 2. Similar illustration is provided in [26, Fig.3] and is replicated here for convenience of the reader.

the C-band between -1 dB and -4 dB for and for the L-band between -2.5 dB and -8.5 dB. Conversion efficiencies are reduced as signals gets further from the pump due to increased linear phase-mismatch. This figure seem to agree well with the shape (relative position of maximums is identical) of measured gain spectrum for core 1 and 2 in Fig. 5 c).

C. Estimation of coupling coefficient

In order to estimate the coupling coefficient C of the weakly coupled DC-HNLF we inserted CW light in one of the cores of the DC-HNLF, for example core 1 and made power measurements of the light at output of cores 1 and 2. We measured a power difference between cores to be 35 dB. The power flows from core 1 to core 2 accordingly to the following equations [38, Eq. 4.39 and 4.40]

$$P_1(z) = 1 - F\,sin^2(qz) \tag{2}$$

$$P_2(z) = F\,sin^2(qz) \tag{3}$$

where,

$$q = \sqrt{C^2 + \delta^2}$$

$$\delta = \frac{\beta_a - \beta_b}{2}$$

and

$$F = \frac{1}{1 + \left(\frac{\delta}{C}\right)^2} \tag{4, 5}$$

In order to simplify the estimations we will neglect the wavelength dependent nature of the mismatch δ, between propagation constants β_a and β_b of cores 1 and 2, respectively, i.e., $\beta_a \approx \beta_b$, leading to $F \approx 1$, and $q \approx C$. The powers in cores 1 and 2, i.e., P_1 and P_2, respectively, propagate along the propagation distance z. We solve equations (2) and (3), by setting $10\log_{10}\left(\frac{P_1(L)}{P_2(L)}\right) = 35$, where $L = 300$ m is the total length of the fiber. This leads the coupling coefficient to be,

$$C = 5.93 \times 10^{-5}\,\mathrm{m}^{-1}, \tag{6}$$

which is typically above from what has been estimated in standard homogeneous multicore fibres [39].

IV. Discussion

It is noticeable from Fig. 4 b) and confirmed by Fig.5 c) that core 1 and 2 have somewhat distinct ZDWs, i.e. more specifically they have 5 nm difference. If the cores are weakly-coupled this can be circumvented by launching two pumps with distinct wavelengths matching the ZDW of the individual cores. This work intended to design a new type of fiber that due to claimed resilience to environmental conditions [27], could be used for several diversity schemes in a variety of dimensions (polarization, space), for all-optical signal processing applications. The nonlinearity obtained for both cores of this fiber is the one for which the fiber was designed and more important the nonlinearity for so called core 1 and core 2 is very identical. The ZDWs of both cores are close enough to claim that this is indeed a successful realization of a DC-HNLF, taking into account the aforementioned objectives of this work.

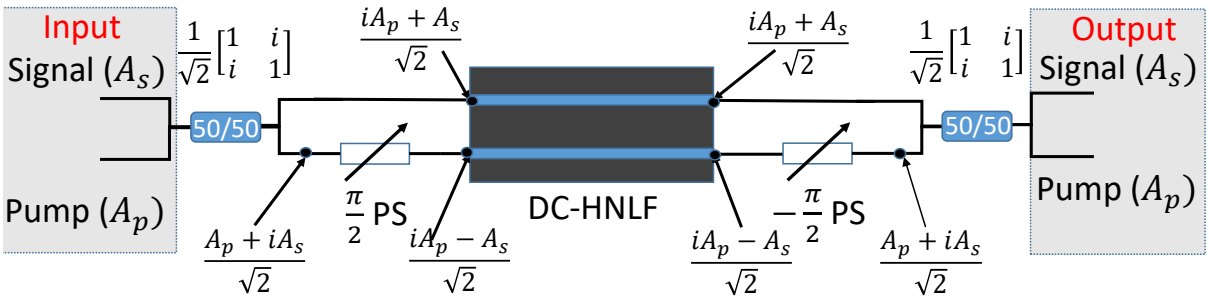

Fig. 8. Simulation setup. PS-phase-shifter

It is worth to discuss the case when the cores are coupled and the impact of having distinct ZDWs for the cores, regarding previous studies on coupled core fibre optical parametric amplifiers [15], [16]. While in the coupled core case it may be desirable, that the ZDW of the individual cores match, it is not a condition to obtain the gain flatness of the DC-FOPA discussed in [15], [16]. The proper placement of the pump after knowing the ZDW of the individual cores can do partially the trick. To show this, we implement a conceptual simulation setup shown in Fig. 8. In this setup the signal and the pump are combined by a $50/50$ coupler and while the signal+pump fields, that go to core 2 is phase-shifted $\pi/2$, the signal (A_s)+pump (A_p) fields that goes to core 1 is inserted directly in the fiber core. This is done so, in order that pumps in both cores are phase aligned and signal fields are in opposite phase. This is the case where the best noise properties for the DC-FOPA are achieved as explained in [16]. Moreover due to similar concept to twin-wave scheme [40], 1^{st} nonlinear crosstalk (XT) noise cancellation, is achieved after coupling both fiber core ends by another $50/50$ coupler, where one of the arms of the interferometer is shifted by $-\pi/2$ radians.

To note that if the fields are coherently aligned, the pump will be filtered out naturally by the interferometer and leave one of the outputs of the $50/50$ coupler, while the signal will leave in the other $50/50$ coupler output. The model of the coupled DC-HNLF is as show in (7),

$$M = i\begin{pmatrix} k_1 - C & \frac{P_p\gamma}{2} & C & 0 \\ -\frac{P_p\gamma}{2} & C - k_1 & 0 & -C \\ C & 0 & k_2 - C & \frac{P_p\gamma}{2} \\ 0 & -C & -\frac{P_p\gamma}{2} & C - k_2 \end{pmatrix} \tag{7}$$

where,

$$\frac{dA(z)}{dz} = MA(z) \tag{8}$$

is the differential equation governing the system of coupled wave equations, z is the propagation length and $A(z) = [A_{s_1}(z), A_{i_1}(z), A_{s_2}(z), A_{i_2}(z)]^T$. The fields $A_{s_{1,2}}(z)$ and $A_{i_{1,2}}(z)$ are the signal and idler fields in core 1 and 2, respectively. M is the matrix of coefficients resultant from a 4-wave coupled equation, where C is the linear coupling coefficient responsible for the coupling coefficient between cores. To note that the formal definition of $C = \frac{\frac{\pi}{2}}{L_c}$, where L_c is the coupling length and is wavelength dependent. We neglect this wavelength dependence of the coupling coefficient. This dependence leads to a coupling coefficient induced dispersion [22]. Nevertheless previous studies have shown the negligible impact of this dependence on the modulation instability spectrum, when the input waves inserted in the cores have equal power and are counter or co-phased [22]. This is exactly the case studied here. Matrix (7) is identical to the one presented in [15] for which derivation was detailed in [16], however we generalize it to admit distinct dispersion parameters in both cores represented by k_1 and k_2, as defined in (9),

$$\begin{aligned} k_1 &= \gamma P_p/2 + S_3\Delta\lambda_1\lambda.^2 \\ k_2 &= \gamma P_p/2 + S_3\Delta\lambda_2\lambda.^2 \end{aligned} \tag{9}$$

where γ is the nonlinear parameter of the individual cores, P_p is the power of the pump equally divided by both cores, $\Delta\lambda_{1,2} = \lambda_{0_{1,2}} - \lambda_p$, with $\lambda_{0_{1,2}}$ the ZDW of cores 1 and 2, respectively, λ_p is the wavelength of the pump, λ is the wavelength of the signal and $S_3 = (2\pi c)^3/\lambda_p^6\beta_3(\lambda_p)/2$ is the conversion factor from frequency (rad/s) to wavelength domain. In this study only 2^{nd} order dispersive effects are included in the model and therefore β_4 is neglected. The solution of (8) is given by (10)

$$A(z) = e^{Mz}A(0). \tag{10}$$

where $A(0) = [A_{s_1}(0), A_{i_1}(0), A_{s_2}(0), A_{i_2}(0)]^T = [\sqrt{2}/2, 0, -\sqrt{2}/2, 0]^T$. By obtaining the solution of (10) we

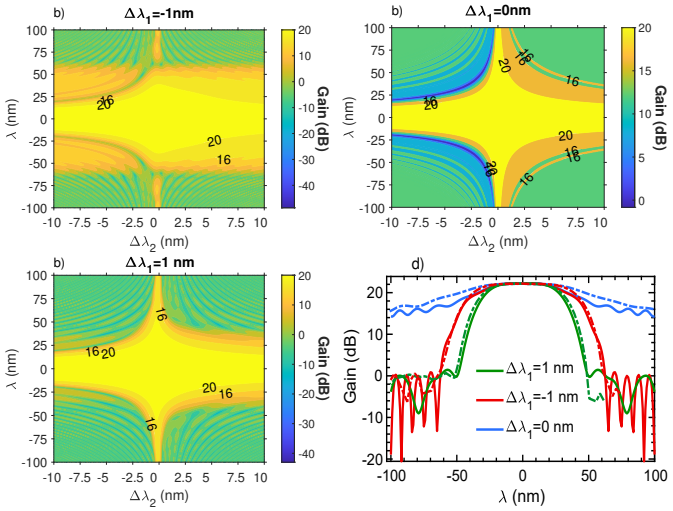

Fig. 9. Varying pump wavelength shifting in respect to λ_{0_2}, against wavelength of the signal and gain of the coupled DC-FOPA, represented in isolines, when wavelength shifting respect to λ_{0_1} is a) $\Delta\lambda_1 = -1$ nm, b) $\Delta\lambda_1 = 0$ nm c) $\Delta\lambda_1 = 1$ nm. In d) gain spectrum for $\Delta\lambda_2 = 2$ nm for $\Delta\lambda_1 = -1, 0, 1$ nm. Solid curve is the solution of (10) and dashed-dot curved is the SSFT solver of the NLSE.

obtain the gain of the system described in Fig. 8 with (11),

$$Gain = \frac{|A_s(z)|^2}{|A_s(0)|^2}, \tag{11}$$

where $A_s(z) = \frac{A_{s_1}(z) - A_{s_2}(z)}{\sqrt{2}}$.

In order to get insight into the problem we set $Pp = 10$ W and the length of the fiber to $z = 100$ m , $\gamma = 6.5$ W^{-1} km^{-1}, $C = \frac{\gamma P_p}{4}$ and $\beta_3 = 0.06$ ps^3/km. The chosen value of the coupling coefficient C, was discussed previously in [15], [16]. The objective to set C to this value is as follows, i.e., in order to have the maximum, flat and exponential gain evolution over the length of the fiber, it is required to tune the coupling coefficient, by approximating the cores, to match the nonlinear phase-mismatch, which is given by $k_{NL} = \frac{P_p \gamma}{2}$ [15], [16]. The phase-mismatch between supermodes is given by $2C$ [21] and assuming $C = \frac{P_p \gamma}{4}$, this cancels k_{NL}. Having this note in mind we plotted isolines of the gain, where it was fixed $\Delta\lambda_1$ and varied $\Delta\lambda_2$ with λ. The results are shown in Fig. 9.

In Fig. 9 the yellow part in the center of the plots describes where the gain is flat over a certain bandwidth depending on the $\Delta\lambda_2$, i.e. the shift of the pump in respect to the ZDW of core 2. It is seen that depending on $\Delta\lambda_1$ there is a specific behavior, but a common denominator is that more bandwidth is obtained when the pump is located in the core ZDW with the shorter wavelength, letting the other core, i.e. in this case core 2, to be in the normal dispersion regime, i.e. $\Delta\lambda_2 > 0$ nm. Therefore it shall be possible to tune λ_p in order to have the best performance possible. It is evident in Fig. 9 b) that the bandwidth of the DC-FOPA is roughly inversely proportional to the difference between ZDW of core 1 and 2, however the impact of the difference depends on the sign of $\Delta\lambda_2$, i.e., if it is set to be in the normal dispersion regime $\Delta\lambda_2 > 0$ or otherwise anomalous dispersion regime $\Delta\lambda_2 < 0$. Fig. 9 d) shows some gain spectrum examples, for $\Delta\lambda_1 = -1, 0, 1$ nm, where we see that if the pump is located in the ZDW of core 1 while the $\Delta\lambda_2 = 0$ nm, this results in the widest gain spectrum bandwidth possible. It seems that in this case, that the phase-matching condition does not drop suddenly like in the other cases, but instead drops smoothly and that some periodic ripple occurs in the gain spectrum. There is possibly a balancing phase-matching condition provided by the interplay between coupling and distinct dispersive phase-mismatch, made available individually by the cores. Fig. 9 d) also shows matching curves with split step Fourier transform (SSFT) solver of two identical coupled cores where the electric fields slowly varying envelope evolution is described by two coupled nonlinear Shrödinger equations (NLSEs)

$$\begin{aligned} \frac{\partial U_1}{\partial z} &= i\sum_{n=2}^{\infty} i^n \frac{\beta_n}{n!}\frac{\partial^n U_1}{\partial t^n} + i\gamma U_1|U_1|^2 + iCU_2 \\ \frac{\partial U_2}{\partial z} &= i\sum_{n=2}^{\infty} i^n \frac{\beta_n}{n!}\frac{\partial^n U_2}{\partial t^n} + i\gamma U_2|U_2|^2 + iCU_1, \end{aligned} \tag{12}$$

where $U_{1,2}$ are the two field amplitudes defined in a co-moving temporal reference frame of coordinate t and evolving along spatial coordinate z. β_n is the n-th order dispersion coefficient. If we set the linear and nonlinear operators as $D_k = i\sum_{n=2}^{\infty} i^n \frac{\beta_n}{n!}\frac{\partial^n}{\partial t^n}$ and $N_k = i\gamma|U_k|^2$ where k is the core index number, the SSFT method solves Eqs.(12) by giving the solution of the DC-HNLF at each interval dz, and coupling them by a 2x2 coupler transfer matrix R given by [41]:

$$R = \begin{pmatrix} \cos(Cdz) & i(Cdz) \\ i(Cdz) & \cos(Cdz) \end{pmatrix}. \tag{13}$$

To note that R is the solution of (12) neglecting the respective D_k and N_k operators. At each step dz the solution of Eqs.(12) is given by

$$\begin{pmatrix} U_1(z+dz) \\ U_2(z+dz) \end{pmatrix} \approx R \begin{pmatrix} e^{D_1 dz/2} e^{N_1 dz} e^{D_1 dz/2} U_1(z) \\ e^{D_2 dz/2} e^{N_2 dz} e^{D_2 dz/2} U_2(z) \end{pmatrix}. \tag{14}$$

We see a very good agreement between the solution of (12) and the analytical solution of (10). The general conclusion of this section is that distinct ZDW between cores is undesirable and it will reduce bandwidth of coupled DC-FOPA, but it can be managed in order to get the best performance possible, while still allowing broad bandwidth, by setting the pump to be located closer to the core ZDW with shorter wavelength and letting the other core operate in the normal dispersion regime.

V. Conclusions

In this paper it was shown the characterization of a custom manufactured dual-core highly nonlinear fiber (DC-HNLF), for all-optical signal processing applications. We demonstrated all-optical wavelength conversion and parametric amplification in a DC-HNLF. We obtained a fiber with an effective nonlinear parameter of 6.6 W^{-1} km^{-1} and 6.3 W^{-1} km^{-1}, for core 1 and 2, respectively, however we obtained cores with distinct dispersion profile. While in the weakly-coupled DC-HNLF it is possible to tune the pump wavelengths to match the distinct zero-dispersion wavelength (ZDW), numerical analysis shows that if the cores are coupled and have distinct ZDW it is possible to tune the wavelength of the pump to obtain the best performance possible at the expense of reducing bandwidth. Further experiments will show the possibility to explore this structure for wide-band parametric amplification.

VI. Acknowledgements

Lille Aston- Ferrara- international project on advanced nonlinear effects in optical fibers (LAFONI) is acknowledged.

We acknowledge the Aston University managed projects EP/S016171/1 EPSRC-SFI: Energy Efficient M Communication using Combs (EEMC) and EP/S003436/1 Photonic Phase Conjugation Systems (PHOS). This work is funded by FCT/MCTES through national funds and when applicable co-funded EU funds under the project UIDB/50008/2020-UIDP/50008/2020. This work was also partially supported by the French Ministry of Higher Education and Research; the Hauts de-France Regional Council and the European Regional Development Fund (ERDF) through the Contrat de Projets Etat-Region (C.P.E.R. Photonics for Society, P4S) Vitor Ribeiro wants to acknowledge Auro M.Perego from Aston university for insightful discussions about this work. We also want to

acknowledge the time given voluntarily by the anonymous reviewers to read our paper and provide useful suggestions in order to improve it.

REFERENCES

[1] A. A. Maĭer, "Optical transistors and bistable devices utilizing nonlinear transmission of light in systems with undirectional coupled waves," *Sov. J. Quantum Electron.*, vol. 12, no. 11, p. 1490, Nov. 1982.

[2] S. M. Jensen, "The nonlinear coherent coupler," *IEEE Trans. Microw. Theory Tech.*, vol. 30, no. 10, pp. 1568–1571, Oct. 1982.

[3] S. Trillo, S. Wabnitz, E. M. Wright, and G. I. Stegeman, "Soliton switching in fiber nonlinear directional couplers," *Opt. Lett., OL*, vol. 13, no. 8, pp. 672–674, Aug. 1988.

[4] S. R. Friberg, A. M. Weiner, Y. Silberberg, B. G. Sfez, and P. S. Smith, "Femotosecond switching in a dual-core-fiber nonlinear coupler," *Opt. Lett.*, vol. 13, no. 10, pp. 904–906, Oct. 1988.

[5] M. Romagnoli, S. Trillo, and S. Wabnitz, "Soliton switching in nonlinear couplers," *Opt. Quantum Electron.*, vol. 24, no. 11, pp. S1237–S1267, Nov. 1992.

[6] Y. S. Kivshar, "Switching dynamics of solitons in fiber directional couplers," *Opt. Lett., OL*, vol. 18, no. 1, pp. 7–9, Jan. 1993.

[7] A. Mecozzi, "Parametric amplification and squeezed-light generation in a nonlinear directional coupler," *Opt. Lett.*, vol. 13, no. 10, pp. 925–927, Oct 1988. [Online]. Available: http://www.osapublishing.org/ol/abstract.cfm?URI=ol-13-10-925

[8] K.-I. Kitayama, N. Shibata, and M. Ohashi, "Two-core optical fibers: experiment," *J. Opt. Soc. Am. A, JOSAA*, vol. 2, no. 1, pp. 84–89, Jan. 1985.

[9] Z. Wang, T. Taru, T. A. Birks, J. C. Knight, Y. Liu, and J. Du, "Coupling in dual-core photonic bandgap fibers: theory and experiment," *Opt. Express*, vol. 15, no. 8, pp. 4795–4803, Apr 2007. [Online]. Available: http://www.opticsexpress.org/abstract.cfm?URI=oe-15-8-4795

[10] M. Longobucco, I. Astrauskas, A. Pugžlys, D. Pysz, F. Uherek, A. Baltuška, R. Buczyński, and I. Bugár, "Broadband self-switching of femtosecond pulses in highly nonlinear high index contrast dual-core fibre," *Opt. Commun.*, vol. 472, p. 126043, Oct. 2020.

[11] L. Curilla, I. Astrauskas, A. Pugzlys, P. Stajanca, D. Pysz, F. Uherek, A. Baltuska, and I. Bugar, "Nonlinear performance of asymmetric coupler based on dual-core photonic crystal fiber: Towards sub-nanojoule solitonic ultrafast all-optical switching," *Optical Fiber Technology*, vol. 42, p. 39, May 2018.

[12] V. H. Nguyen, Le Xuan The Tai, I. Bugar, M. Longobucco, R. Buczyński, B. A. Malomed, and M. Trippenbach, "Reversible ultrafast soliton switching in dual-core highly nonlinear optical fibers," *Opt. Lett., OL*, vol. 45, no. 18, pp. 5221–5224, Sep. 2020.

[13] Z. Lian, P. Horak, X. Feng, L. Xiao, K. Frampton, N. White, J. A. Tucknott, H. Rutt, D. N. Payne, W. Stewart, and W. H. Loh, "Nanomechanical optical fiber," *Opt. Express*, vol. 20, no. 28, pp. 29 386–29 394, Dec 2012. [Online]. Available: http://www.opticsexpress.org/abstract.cfm?URI=oe-20-28-29386

[14] Z. Ye, P. Zhao, K. Twayana, M. Karlsson, V. Torres-Company, and P. A. Andrekson, "Overcoming the quantum limit of optical amplification in monolithic waveguides," *Sci Adv*, vol. 7, no. 38, p. eabi8150, Sep. 2021.

[15] V. Ribeiro, M. Karlsson, and P. Andrekson, "Parametric amplification with a dual-core fiber," *Opt. Express*, vol. 25, no. 6, pp. 6234–6243, Mar. 2017.

[16] V. Ribeiro, A. Lorences-Riesgo, P. Andrekson, and M. Karlsson, "Noise in phase-(in) sensitive dual-core fiber parametric amplification," *Opt. Express*, vol. 26, no. 4, pp. 4050–4059, 2018.

[17] H. Zhu, Z. Zhu, L. Yu, L. Cheng, Y. Zhang, H. Sui, S. Taccheo, and J. Peng, "One-pump phase sensitive fiber optical parametric amplifier with dual-core fiber," *IEEE Journal of Selected Topics in Quantum Electronics*, vol. 26, no. 4, pp. 1–5, 2020.

[18] J. Zhou, Q. Hu, J. Wu, and W. Chen, "Dual-core fiber optical parametric amplifiers with a general pump configuration," *IEEE Photonics Technology Letters*, vol. 30, no. 1, pp. 19–22, 2018.

[19] V. Ribeiro and A. M. Perego, "Parametric amplification in lossy nonlinear waveguides with spatially dependent coupling," *Opt. Express*, vol. 30, no. 10, pp. 17 614–17 624, May 2022. [Online]. Available: http://opg.optica.org/oe/abstract.cfm?URI=oe-30-10-17614

[20] V. Ribeiro and A. Perego, "Theory of parametric amplification in coupled lossy waveguides," in *Conference on Lasers and Electro-Optics*. Optical Society of America, 2022, p. JTh3A.12.

[21] M. J. Li and T. Hayashi, "Advances in low-loss, large-area, and multicore fibers," *Optical Fiber Telecommunications VII*, pp. 3–50, 1 2019.

[22] J. H. Li, K. S. Chiang, and K. W. Chow, "Modulation instabilities in two-core optical fibers," *J. Opt. Soc. Am. B*, vol. 28, no. 7, pp. 1693–1701, Jul 2011. [Online]. Available: http://www.osapublishing.org/josab/abstract.cfm?URI=josab-28-7-1693

[23] F. S. Yang, M. C. Ho, M. E. Marhic, and L. G. Kazovsky, "Demonstration of two-pump fiber optical parametric amplification," in *Conference Proceedings. LEOS '97. 10th Annual Meeting IEEE Lasers and Electro-Optics Society 1997 Annual Meeting*, vol. 1. ieeexplore.ieee.org, Nov. 1997, pp. 122–123 vol.1.

[24] F. S. Yang, M. C. Ho, E. Marhic, and L. G. Kazovsky, "Demonstration of two-pump fibre optical parametric amplification," *Electron. Lett.*, vol. 33, no. 21, pp. 1812–1813, 1997.

[25] G. P. Agrawal, "Nonlinear fiber optics," in *Nonlinear Science at the Dawn of the 21st Century*. Springer, 2000, ch. 10, pp. 394–399.

[26] A. D. Szabo, V. Ribeiro, C. B. Gaur, A. A. I. Ali, A. Mussot, Y. Quiquempois, G. Bouwmans, and N. J. Doran, "Dual-polarization c+l-band wavelength conversion in a twin-core highly nonlinear fibre," *OFC 2021 Virtual conference, Paper MB5.4*, 2021.

[27] R. S. Luís, B. J. Puttnam, J.-M. Delgado Mendinueta, W. Klaus, Y. Awaji, and N. Wada, "Comparing inter-core skew fluctuations in multi-core and single-core fibers," in *2015 Conference on Lasers and Electro-Optics (CLEO)*, 2015, pp. 1–2.

[28] CIENA, "Dtm-100g, coherent 100g transponder module," https://www.ciena.com/__data/assets/pdf_file/0015/23631/DTM-100G_DS.pdf, 2019.

[29] F. Yaman, Q. Lin, and G. P. Agrawal, "A novel design for polarization-independent single-pump fiber-optic parametric amplifiers," *IEEE Photonics Technology Letters*, vol. 18, no. 22, pp. 2335–2337, 2006.

[30] B. Jaramillo Ávila, J. M. Torres, R. d. J. León-Montiel, and B. M. Rodríguez-Lara, "Optimal crosstalk suppression in multicore fibers," *Sci. Rep.*, vol. 9, no. 1, p. 15737, Oct. 2019.

[31] L. Gruner-Nielsen, "Polarization maintaining highly nonlinear fibers and their applications," in *2009 IEEE/LEOS Winter Topicals Meeting Series*, 2009, pp. 239–240.

[32] "Optical spectrum analyzer setting guidelines for pulsed light measurement — yokogawa test & measurement corporation," https://tmi.yokogawa.com/library/resources/application-notes/optical-spectrum-analyzer-setting-guidelines-for-pulsed-light-measurement/Yokogawa optical spectrum analyzer website.

[33] V. Gordienko, M. F. C. Stephens, and N. J. Doran, "Broadband gain-spectrum measurement for fiber optical parametric and raman amplifiers," *IEEE Photonics Technology Letters*, vol. 29, no. 16, pp. 1399–1402, 2017.

[34] J. Chavez Boggio, F. Callegari, S. Tenenbaum, H. Fragnito, J. Rosolem, and M. debarros, "Demonstration of 26 db on-off gain of a two-pump fiber optical parametric amplifier," in *Optical Fiber Communication Conference and Exhibit*, 2002, pp. 636–637.

[35] M. Karlsson, "Transmission systems with low noise phase-sensitive parametric amplifiers," *Journal of Lightwave Technology*, vol. 34, no. 5, pp. 1411–1423, 2016.

[36] G. Kalogerakis, K. Shimizu, M. Marhic, K.-Y. Wong, K. Uesaka, and L. Kazovsky, "High-repetition-rate pulsed-pump fiber opa for amplification of communication signals," *Journal of Lightwave Technology*, vol. 24, no. 8, pp. 3021–3027, 2006.

[37] D. Marcuse, C. Manyuk, and P. Wai, "Application of the manakov-pmd equation to studies of signal propagation in optical fibers with randomly varying birefringence," *Journal of Lightwave Technology*, vol. 15, no. 9, pp. 1735–1746, 1997.

[38] K. Okamoto, "Chapter 4 - coupled mode theory," in *Fundamentals of Optical Waveguides (Second Edition)*, second edition ed., K. Okamoto, Ed. Burlington: Academic Press, 2006, pp. 159–207. [Online]. Available: https://www.sciencedirect.com/science/article/pii/B9780125250962500052

[39] M. Koshiba, K. Saitoh, K. Takenaga, and S. Matsuo, "Multi-core fiber design and analysis: coupled-mode theory and coupled-power theory," *Opt. Express*, vol. 19, no. 26, pp. B102–B111, Dec 2011. [Online]. Available: http://opg.optica.org/oe/abstract.cfm?URI=oe-19-26-B102

[40] X. Liu, A. R. Chraplyvy, P. J. Winzer, R. W. Tkach, and S. Chandrasekhar, "Phase-conjugated twin waves for communication beyond the kerr nonlinearity limit," *Nat. Photonics*, vol. 7, no. 7, pp. 560–568, May 2013.

[41] B.-S. Kim, Y. Chung, and S.-H. Kim, "Split-step time-domain analysis of optical waveguide devices composed of a directional coupler and gratings," *Opt. Lett.*, vol. 25, no. 8, pp. 530–532, Apr 2000. [Online]. Available: http://opg.optica.org/ol/abstract.cfm?URI=ol-25-8-530